Photo-assisted electrocatalytic reduction of CO2: A new strategy for reducing catalytic overpotentials

Article

Accepted Version

RESEARCH ARTICLE

Photo-assisted Electrocatalytic Reduction of CO_2: A New Strategy for Reducing Catalytic Overpotentials

James O. Taylor[a], Yibo Wang,[a] and František Hartl*[a]

Abstract: Electrochemical and photochemical reduction of CO_2 are both well-established, independent catalytic routes toward producing added-value chemicals. The potential for any cross-reactivity has, however, hardly been explored so far. In this report, we assess a system primarily using spectroelectrochemical monitoring, where photochemistry assists the cathodic activation of precursor complexes [Mn(CO)$_3$(2,2'-bipyridine)Br] and [Mo(CO)$_4$(6,6'-dimethyl-2,2'-bipyridine)] to lower the catalytic overpotential needed to trigger the electrocatalytic reduction of CO_2 to CO. Following the complete initial 1e$^-$ reduction of the parent complexes, the key photochemical cleavage of the Mn–Mn and Mo–CO bonds in the reduction products, [Mn(CO)$_3$(2,2'-bipyridine)]$_2$ and [Mo(CO)$_4$(6,6'-dimethyl-2,2'-bipyridine)]$^{\bullet-}$, respectively, generates the 2e$^-$-reduced, 5-coordinate catalysts, [Mn(CO)$_3$(2,2'-bipyridine)]$^-$ and [Mo(CO)$_3$(6,6'-dimethyl-2,2'-bipyridine)]$^{2-}$ appreciably closer to the initial cathodic wave R1. Experiments under CO_2 confirm the activity of both electrocatalysts under the photoirradiation with 405-nm and 365-nm light, respectively. This remarkable achievement corresponds to a *ca.* 500 mV positive shift of the catalytic onset compared to the exclusive standard electrocatalytic activation.

Introduction

The recent environmental concerns stemming from the anthropogenic emission of CO_2 is the main driving force behind academic efforts to develop both homogeneous and heterogenous catalytic systems converting CO_2 into valuable chemicals.[1] These systems can broadly be classified as either electrocatalytic[2], photocatalytic[3] or photoelectrocatalytic[4]. In all three cases transition metal α-diimine complexes have emerged as the leading class of catalytic systems, boasting both high levels of selectivity and activity.[5–7] [Re(CO)$_3$(bipy)Cl] (bipy = 2,2'-bipyridine), is a prime example, having first been identified as an electrocatalyst by Lehn and co-workers [8], and two decades later as a photocatalyst by Ishitani and co-workers[9]. The way in which the Re(I) polypyridyl field has developed highlights one of the discernible flaws in the current approach; catalysts are always explored independently as either a photocatalyst or an electrocatalyst. This leads to the primary goal of this report, which is to investigate the possibility of combining the electrochemical reactivity of a catalyst precursor with the photochemical reactivity of its singly reduced intermediates, Schemes 1 and 2. The expectation is that the active 2e$^-$-reduced catalyst can be produced and maintained active at a lower overpotential close to its reoxidation. To our knowledge, this is a unique, yet unexplored way to address the sometimes rather negative reduction potentials along the reduction path of these complexes needed to generate the electrocatalyst, which we have termed as *photo-assisted electrochemical reduction*. In recent years, catalysts based on the unsustainable Earth-rare metals (Re, Ru, Rh, Ir)[2] have been relegated to benchmark status, as the community refocuses efforts on the Earth-abundant metals such as Mn[10–15], Fe[16–18] and more recently the Group-6 triad (Cr, Mo, W).[19–26] For this reason, two viable catalyst precursors, *fac*-[Mn(CO)$_3$(bipy)Br] (**1**) and [Mo(CO)$_4$(6,6'-dmbipy)] (6,6'-dmbipy = 6,6'-dimethyl-2,2'-bipyridine) (**2**) have been selected for this investigation. In the very first reports, the reduction of [Mn(CO)$_3$(bipy)Br] in dry organic solvents was noted to trigger no electrocatalytic CO_2 conversion.[27] It was not until Deronzier[10], and later Kubiak[12], and their co-workers revealed that the presence of small amounts (typically 5%) of Brønsted or Lewis acids were required for an efficient catalytic reaction to occur, that any serious attention was devoted to the Mn-based family of catalysts. Despite a similar molecular structure, [Mn(CO)$_3$(bipy)Br] exhibits a quite different electrochemical reactivity to its Re-analogue. [Mn(CO)$_3$(bipy)Br] initially undergoes 1e$^-$ reduction (at the cathodic wave R1) to the corresponding, unstable radical anion that quickly loses Br$^-$ to form a 5-coordinate radical. As the radical is reducible at less negative potentials than the parent compound, it quickly converts electrochemically (ECE) to the 5-coordinate anion, [Mn(CO)$_3$(bipy)]$^-$. At this stage the 5-coordinate anion reacts via zero-electron coupling with the yet unreduced parent to form [Mn(CO)$_3$(bipy)]$_2$. The resulting dimer must be reduced at more negative potentials to recover the 5-coordinate anion (at the cathodic wave R(D)). The dominant catalytic response of CO_2 converting to CO is seen at R(D), coinciding with the formation of the [Mn(CO)$_3$(bipy)]$^-$ catalyst. In selected cases (for 4,4'-dmbipy replacing the bipy ligand), some catalytic response was actually noted[10] already at R1, and there is now a convincing evidence for a second catalytic pathway based on the Mn–Mn dimer.[11,28] Ideally, [Mn(CO)$_3$(bipy)]$^-$ should remain stable at R1, avoiding the secondary dimerization. Kubiak and co-workers succeeded to eliminate the dimerization by introducing bulky 6,6'-dimesityl-bipy (6,6'-mesbipy) into the catalyst.[29,30] However, the catalytic response was not seen at R1, but shifted to more negative potentials where the undesired, stable Mn(I)-bicarbonate product is reduced. This is a case that advocates for the use of photo-assisted electrochemical reduction. A potential complication is, to our knowledge, only the photochemistry of parent

[a] J. O. Taylor, Y. Wang, Prof. Dr. F. Hartl

Department of Chemistry
University of Reading
Whiteknights, Reading, RG6 6AD
United Kingdom
E-mail: f.hartl@reading.ac.uk

Supporting information for this article is given via a link at the end of the document.

Scheme 1: Cathodic pathway of **1** under ambient conditions. The photo-assisted electrochemical reduction is highlighted in green.

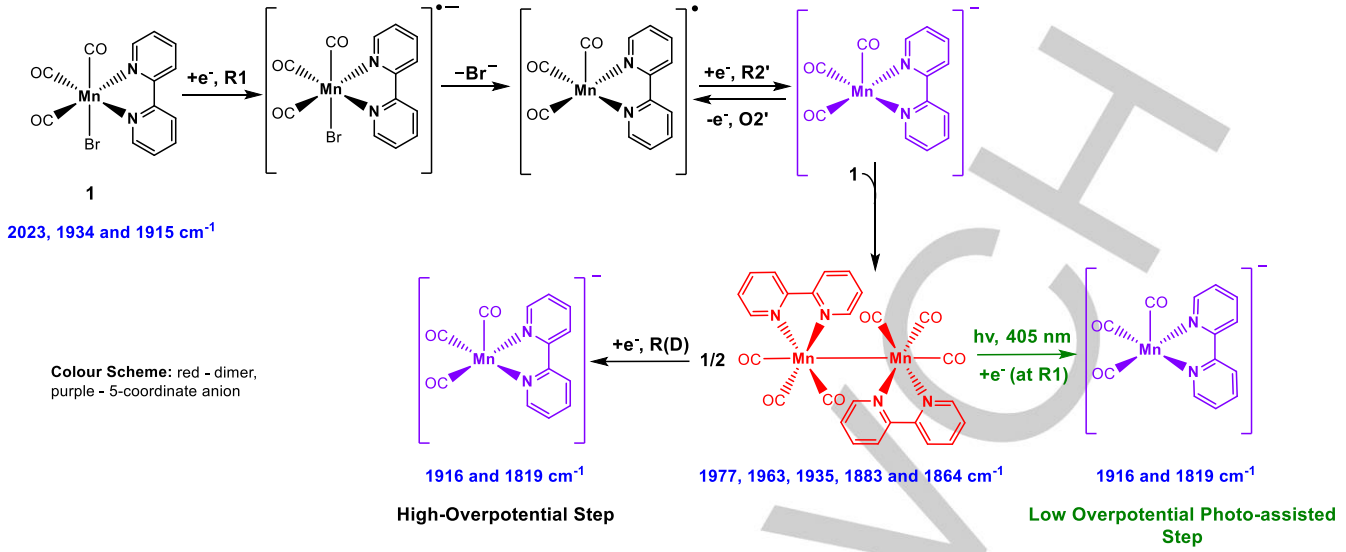

$[Mn(CO)_3(bipy)Br]$ is known, which undergoes fac-to-mer isomerisation followed by optical population of an LLCT/MLCT excited state, Mn–Br bond cleavage and dimer formation.[31] The photochemistry of the dimer $[Mn(CO)_3(bipy)]_2$ has not been extensively investigated, but it was exploited in the past by Ishitani[28], while the photochemistry of the related dimers $[(Mn(CO)_5]_2$ and $[(CO)_3(bipy)Mn–Mn(CO)_5]$ was investigated more thoroughly.[32–35] Optical excitation of these dimers with photons of ca. 400-nm wavelength results, through various means, in the population of a dissociative $^3\sigma_{MM}\sigma_{MM}^*$ excited state, which induces homolysis of the Mn–Mn bond and, in turn, yields the corresponding 5-coordinate Mn radicals. Experimental and theoretical studies of closely related $[Re(CO)_3(bipy)]_2$ have revealed[36] that there is no low-lying σ_{MM}^* orbital in this dimer and optical excitation in the visible region (400-800 nm) results in population of MLCT excited states, the lowest one corresponding to $\sigma_{MM}(d,p)\rightarrow\pi^*(bipy)$ charge transfer (seen as an intense absorption band at λ_{max} = 808 nm in THF). The quantum yield for the homolysis of the Re–Re bond from the corresponding triplet excited state is very low (< 10^{-5}) in this case.[37] Molecular orbitals with a $\sigma_{MM}^*(d)$ contribution are high-lying (LUMO+8 – as a minor component, LUMO+17, LUMO+27 – as a significant component, and classical LUMO+28) and a more efficient Re–Re bond cleavage therefore requires UV radiation. To summarize, following the electrochemical production of $[Mn(CO)_3(bipy)]_2$, irradiation with photons of a sufficiently high energy to yield the 5-coordinate radicals theoretically allows access to the catalytic agent already at R1, *via* the cathodic conversion of the amply long-lived radical species[36] to the corresponding 5-coordinate anion at this potential (Scheme 1).

The other target complex, $[Mo(CO)_4(6,6'\text{-dmbipy})]$, has only recently been introduced as an electrocatalyst for CO_2 reduction.[19] The first report on this Group-6 metal tetracarbonyl α-diimine family regarded $[Mo(CO)_4(bipy)]$, a catalyst precursor that initially was not considered very promising, as only a very limited catalytic performance was seen at a very negative reduction potential of R2, triggered by the generation of $2e^-$-reduced $[Mo(CO)_3(bipy)]^{2-}$.[21] It was later discovered that this particular family was quite sensitive to the cathodic material employed. On an Au cathode, the catalytic onset becomes shifted to a much less negative overpotential; in addition, sterically demanding substituents on bipy together with solvent variation can further improve the catalytic performance.[25] The initial $1e^-$ reduction of $[Mo(CO)_4(6,6'\text{-dmbipy}]$ at R1 produces the stable 6-coordinate radical anion $[Mo(CO)_4(6,6'\text{-dmbipy})]^{\bullet-}$; its irreversible reduction at R2 produces transient $[Mo(CO)_4(6,6'\text{-dmbipy})]^{2-}$ quickly losing CO to yield the active catalyst, $[Mo(CO)_3(6,6'\text{-dmbipy})]^{2-}$. The latter dianion is reoxidized on the reverse anodic scan at O2' to $[Mo(CO)_3(6,6'\text{-dmbipy})]^{\bullet-}$ (Scheme 2). This observation allows one to estimate the position of the forward reduction wave, R2', only scarcely observable directly.[19] The preceding work[19] confirms that when using a Pt cathode, the catalytic response is seen exclusively at R2, while replacement with an Au cathode causes the onset of the catalytic CO_2 reduction to appear in the vicinity of R2'. The origin of this phenomenon has been explained[38] by the co-existence of $[Mo(CO)_4(6,6'\text{-dmbipy})]^{\bullet-}$ with a small amount of $[Mo(CO)_3(6,6'\text{-dmbipy})]^{\bullet-}$. At the Au surface the equilibrium is shifted more toward the 5-coordinate member of the radical pair. As $[Mo(CO)_3(6,6'\text{-dmbipy})]^{\bullet-}$ is reducible to $[Mo(CO)_4(6,6'\text{-dmbipy})]^{2-}$ at R2' < R2, the early onset of the catalytic wave has the origin in the CO dissociation facilitated by the cathodic Au surface. It was tempting to enhance this process with photodissociation, especially at a cathodic Pt surface where it was hardly observed as thermally driven. While the photochemistry of the strongly air- and moisture-sensitive 6-coordinate radical anions is poorly known, the photodissociation of CO from the parent neutral tetracarbonyl complexes is well understood. Under irradiation with UV light (λ_{exc} = 365 nm), the complexes of this type are known to undergo CO-dissociation already from an optically populated ^{1}MLCT state.[39–41] Resonance Raman studies on $[W(CO)_4(bpym)]^{\bullet-}$ (bpym = 2,2'-bipyrimidine) have revealed that the MLCT absorption band becomes blue-shifted compared to the neutral parent compound.[42] However, it has remained open-ended whether the MLCT photoexcitation in the singly reduced

Scheme 2: Cathodic pathway of **2** under ambient conditions. The photo-assisted electrochemical reduction is highlighted in green.

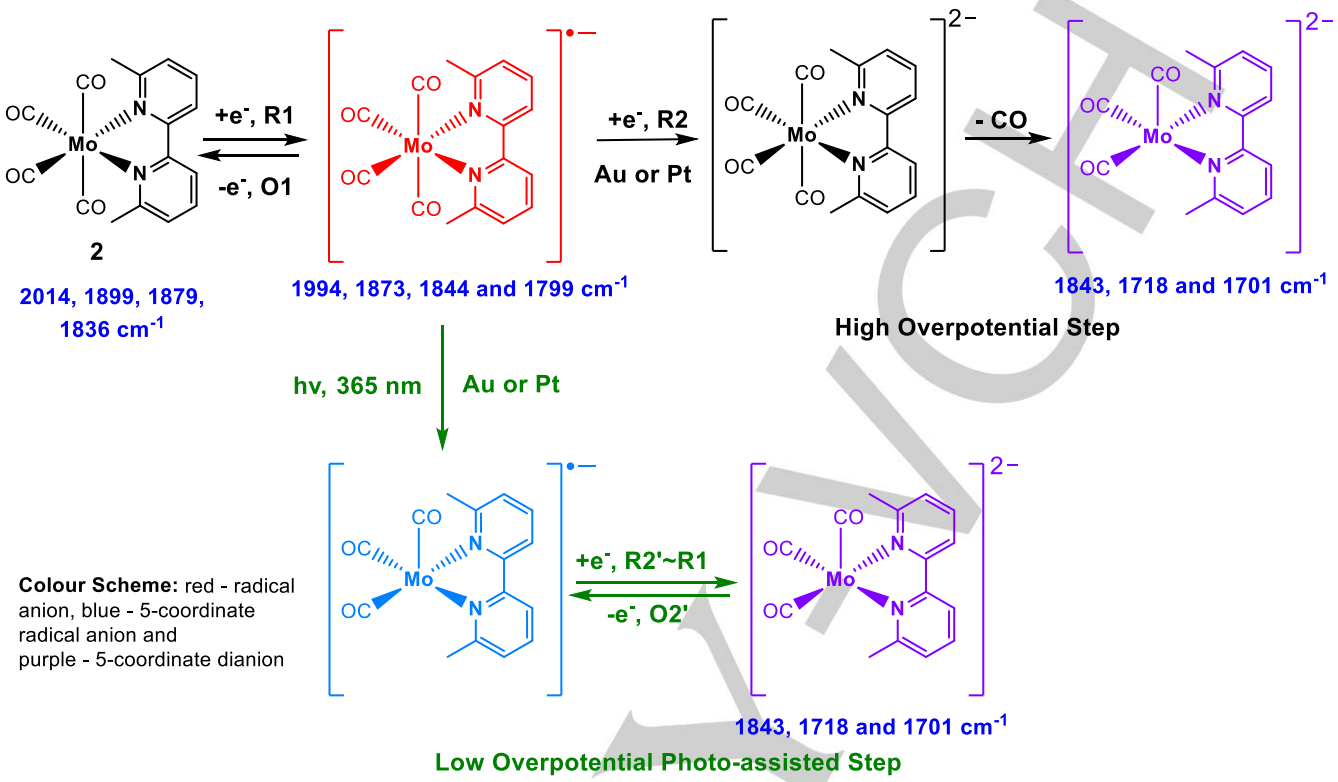

state similarly initiates the CO dissociation to directly generate the 5-coordinate radical anion. The aim of this work is to probe the CO photodissociation from $[Mo(CO)_3(6,6'\text{-dmbipy})]^{\bullet-}$ at the applied cathodic potential of R2' to form the transient $[Mo(CO)_3(6,6'\text{-dmbipy})]^{\bullet-}$ concomitantly reducible to $[Mo(CO)_3(6,6'\text{-dmbipy})]^{2-}$, thereby providing access to the catalytic activation of CO_2 at a considerably reduced overpotential regardless of the cathodic metal surface.

As stated, our primary goal in this study is to investigate the possibility of photo-assisted electrochemical reduction of CO_2 already at, or close to the parent cathodic wave R1, that is, at a significantly reduced overpotential: first, to prove the formation of the catalyst in the absence of CO_2 and then to explore the CO_2 activation under the same conditions. In both selected cases, $[Mn(CO)_3(bipy)Br]$ and $[Mo(CO)_4(6,6'\text{-dmbipy})]$, the negatively shifted second electrochemical reduction step generating the active catalyst was tested for replacement by the controlled photoirradiation, allowing the catalyst to form.

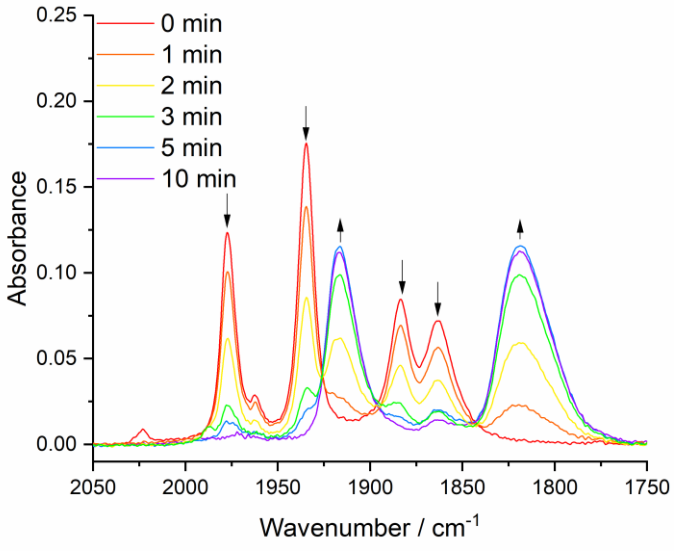

Figure 1. IR SEC monitoring of the photo-assisted electrochemical reduction of **1** at R1, which ultimately yields the 5-coordinate anion $[Mn(CO)_3(bipy)]^-$ (↑), following 405-nm irradiation of electrogenerated $[Mn(CO)_3(bipy)]_2$ (↓) over the course of several minutes. Conditions: THF/TBAH, an OTTLE cell (Pt mesh cathode), T = 298 K.

Results and Discussion

Photo-assisted Electrochemical Reduction of $[Mn(CO)_3(bipy)Br]$ (1)

The primary method of investigation in this report is IR-spectroelectrochemistry at ambient conditions, conducted with a purpose-built OTTLE cell that permits to combine in situ irradiation with a LED source and spectroscopic monitoring of the electrochemistry required for this project. For full experimental details, see Supporting Information.

Table 1. IR absorption data for complexes **1** and **2** and their reduction products. Measured in THF/TBAH within an OTTLE cell.

Complex	v(CO) / cm^{-1}
[Mn(CO)$_3$(bipy)Br] (**1**)	2023, 1934 and 1915
[Mn(bipy)(CO)$_3$(OTf)]	2043 and 1943br
[Mn(CO)$_3$(bipy)]$_2$	1977, 1963, 1935, 1883 and 1864
[Mn(CO)$_3$(bipy)]$^-$	1916 and 1819
[Mo(CO)$_4$(6,6'-dmbipy)] (**2**)	2014, 1899, 1879 and 1836
[Mo(CO)$_4$(6,6'-dmbipy)]$^{\bullet-}$ (**2**$^{\bullet-}$)	1994, 1873, 1844 and 1799
[Mo(CO)4(6,6'-dmbipy-H)]$^-$ [a]	1996, 1874, 1845 and 1798
Unassigned complex [b]	2005, 1885, 1867 and 1829
Unassigned complex [c]	1980, 1864, 1831 and 1784
[Mo(CO)$_3$(6,6'-dmbipy)]$^{2-}$	1843, 1718 and 1701
Unassigned complex [d]	1864 and 1712br

[a] In *N*-methyl-2-pyrrolidone.[19] [b] A tetracarbonyl complex formed upon electrochemical reduction of **2**$^{\bullet-}$ at R2 in THF under CO_2. Most likely an adduct of protonated [Mo(CO)$_4$(6,6'-dmbipy-H)]$^-$ (Ref.[19]) with CO_2. [c] A tetracarbonyl complex formed upon the photo-assisted electrochemical reduction of **2**$^{\bullet-}$ at R2' in THF under CO_2. [d] A tricarbonyl complex formed upon photoirradiation of [Mo(CO)$_3$(6,6'-dmbipy)]$^{2-}$ in THF.

To reiterate from the introductory section, the electrochemical activation of [Mn(CO)$_3$(bipy)Br] (**1**) has been reported extensively. In THF, cyclic voltammetry (Figure SI-1, Supporting Information) reveals two irreversible cathodic waves, R1 ($E_{p,c}$ = -1.91 V vs Fc/Fc$^+$), due to the overall parent-to-dimer conversion (ECEC) process, and R(D) ($E_{p,c}$ = -2.11 V) where the dimer further reduces to maintain the 2e$^-$-reduced [Mn(CO)$_3$(bipy)]$^-$ at the cathode. It is now widely accepted that the latter 5-cooordinate anion is the dominant active electrocatalyst at R(D). IR spectroelectrochemistry, (Figure SI-2, Supporting Information) provides an unambiguous assignment of the reduced species. At R1, the parent-to-dimer reduction is confirmed by the replacement of the v(CO) bands of **1** at 2023, 1934 and 1915 cm^{-1} with five (of the six possible) v(CO) bands of [Mn(CO)$_3$(bipy)]$_2$ at 1977, 1963, 1935, 1883 and 1864 cm^{-1}. While at R(D), two low-lying broad absorbances at 1916 and 1819 cm^{-1} are characteristic of the highly π-delocalized, fluxional 5-coordinate anion.[43] Figure 1 then shows the result of the alternative photo-assisted 2e$^-$ electrochemical reduction experiment at R1. In the first instance, the dimer is electrogenerated from **1** via the same ECEC cathodic path. Then, instead of further increasing the overpotential towards R(D), photoirradiation at 405 nm triggers the conversion of the dimer to the 5-coordinate anion already at R1. The catalyst remains 'locked' in the active 2e$^-$-reduced form, with an additional electrochemical energy cost of further reducing the dimer almost completely negated. The UV-vis absorption spectra of parent **1**, the dimer and the 5-coordinate anion are depicted in Figure SI-3 (Supporting Information). The visible electronic absorption of [M(CO)$_3$(bipy)]$_2$ (M = Mn and Re[36]) is very similar and we consider the same MLCT assignment as reported for M = Re. Irradiation into two separate bands of [Mn(CO)$_3$(bipy)]$_2$ at λ_{max} = 398 and 832 nm was attempted. Only the high-energy excitation with λ_{exc} = 405 nm led to the Mn–Mn bond cleavage, giving access to the dissociative $^3\sigma_{MM}\sigma_{MM}^*$ state. The low-energy excitation most likely populates the $\sigma_{MM}(d)\pi^*$(bipy) charge transfer state with a high energetic barrier to cross the dissociative $^3\sigma_{MM}\sigma_{MM}^*$ state, hence keeping the Mn–Mn bond intact. Comparison of the relative IR v(CO) absorbances of the dimer and [Mn(CO)$_3$(bipy)]$^-$ formed during the standard electrochemical (Figure 1) and photo-assisted (Figure SI-2, Supporting Information) processes at R(D) and R1, respectively, reveals that not all the electrogenerated dimer molecules are converted into the 5-coordinate anion along the photo-assisted route. Instead, upon the 405-nm photoexcitation the dimer seems to follow a parallel photodecarbonylation pathway, which is accounting for the lower

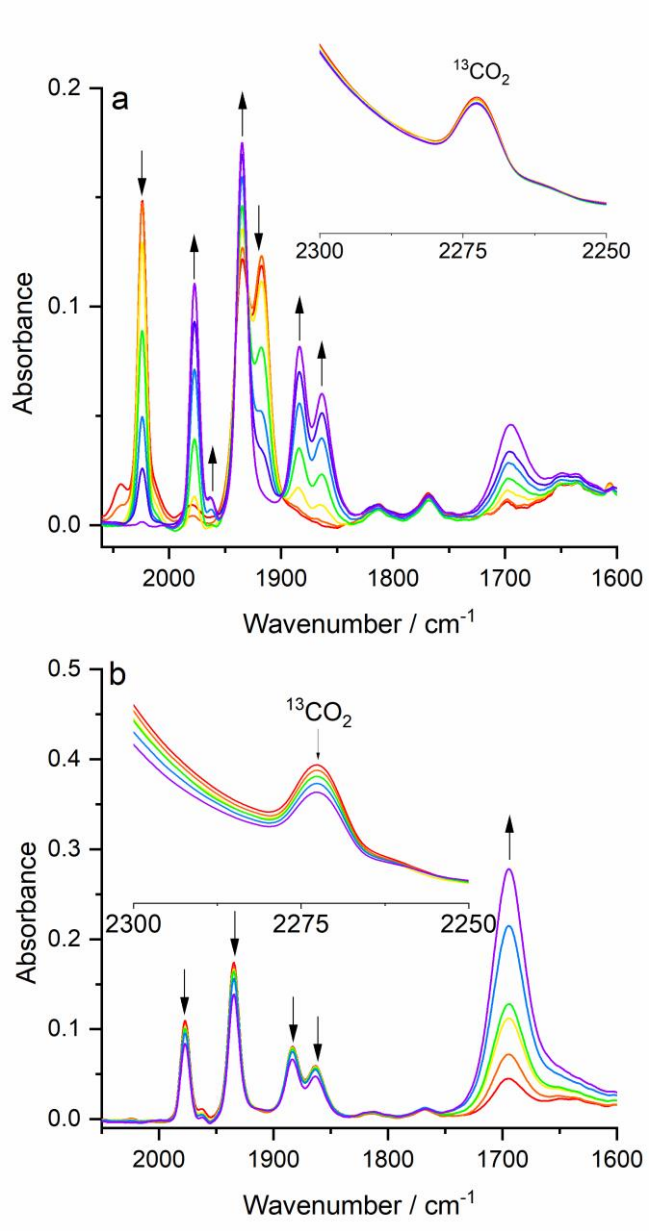

Figure 2. IR SEC monitoring of (a) the standard electrochemical reduction of [Mn(CO)$_3$(bipy)Br] (**1**) (↓) to [Mn(CO)$_3$(bipy)]$_2$ (↑) at R1, and (b) the dimer (↓) to the catalyst [Mn(CO)$_3$(bipy)]$^-$ at R(D) (detectable under argon, cf. Figure SI-4a, Supporting Information)), triggering electrocatalytic reduction of CO_2. Inset: the $^{13}CO_2$ satellite peak used as a reference. Conditions: CO_2-saturated THF/TBAH containing 5% TFE, an OTTLE cell (Pt mesh cathode), T = 298 K.

v(CO) band intensities of the 5-coordinate anion in Figure 1, compared to the IR spectral changes in Figure SI-2 (Supporting Information). Aside from this, in THF, a still significant amount of the dimer is successfully converted to the 5-coordinate anion.[44] The presence of either 5% trifluoroethanol (TFE) or methanol (MeOH) in the Ar-saturated electrolyte does not impact the photo-assisted conversion process at R1 significantly (Figures SI-4 and SI-5, Supporting Information). With CO_2 dissolved in the dry THF/TBAH electrolyte, the 5-coordinate anion can again be produced from the dimer *via* the standard ECE cathodic process at R(D) (Figure SI-6, Supporting Information) or the photo-assisted process at R1 (Figure SI-7, Supporting Information), and no conversion of CO_2 is observed in either case. As expected, the electrocatalytic reduction of CO_2 is observed only with the Brønsted acids (TFE or MeOH) added to the electrolyte. Along the standard electrochemical route, only a limited CO_2 conversion is noticed at R1 (Figure 2 and Figure SI-8 (Supporting Information)), where **1** is again converted to the dimer by the ECEC mechanism. It is only when R(D) is passed and the 5-coordinate anion reformed (but not detected in this case due to its rapid reaction with CO_2) that the electrocatalytic process does begin in earnest, as testified primarily by the decreasing reference satellite $^{13}CO_2$ peak. The primary product of the CO_2 reduction is CO in this case.[10] Another species was also observed, exhibiting a C=O stretch at 1694 cm^{-1} in THF/TFE (Figure 2) or 1665 cm^{-1} in THF/MeOH (Figure SI-8, Supporting Information) so far unreported in the literature to the best of our knowledge. These wavenumbers are attributed to subordinate bicarbonate usually accompanying the main CO product. This assignment is supported by experiments with isotopically labelled $^{13}CO_2$ (Figure SI-9, Supporting Information), which reveal an isotopic shift of almost 50 cm^{-1}, in line with the ^{13}C=O stretch. The varying position of this band in the IR spectra points to an interaction of the bicarbonate side product with the Brønsted acids used. Encouragingly, CO accompanied by bicarbonate, and some formate were formed also during the photo-assisted electrochemical reduction of **1** at R1 in the presence of CO_2/5% TFE (Figure 3) or CO_2/5% MeOH (Figure SI-10, Supporting Information), proving that the electrocatalytic CO_2 reduction occurs successfully at the lower overpotential under these conditions. However, compared to the standard electrocatalytic process at R(D) (Figure 2 and Figure SI-8 (Supporting Information), markedly less CO_2 reacted on the photo-assisted electrocatalytic activation at R1 in the same time interval. At this stage we cannot identify the reason for the observed difference with certainty. However, the somewhat disappointing lower catalytic performance under CO_2 is assumed to be a result of the above-mentioned parallel photo-decomposition reaction of the dimer, which prevents the full recovery of the catalyst in each redox cycle. In this way, the $^{13}CO_2$ experiment was particularly important to exclude any CO that may be produced via photodecarbonylation. If the dimer were photostable in this respect the performance along the standard and photo-assisted electrocatalytic routes should have been comparable. Nevertheless, as a proof of concept, the $[Mn(CO)_3(bipy)]^-$ catalyst is no doubt active at the cathodic wave R1 of precursor **1** in the photo-assisted mode.

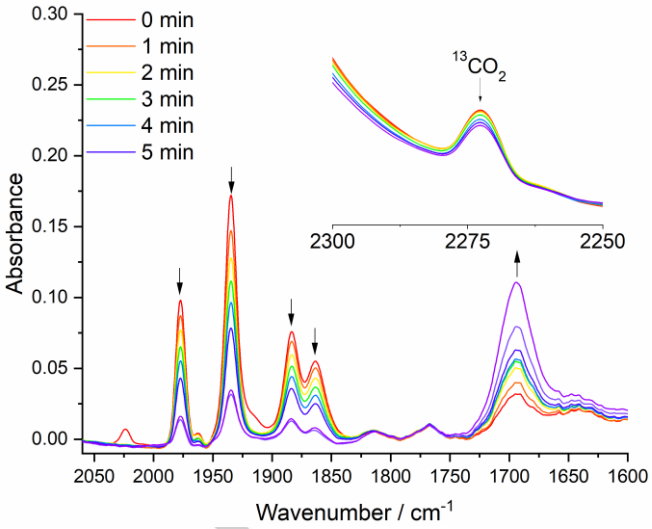

Figure 3. IR SEC monitoring of the photo-assisted electrochemical reduction of $[Mn(CO)_3(bipy)]_2$ (↓) pre-formed from **1** at R1, to the catalyst $[Mn(CO)_3(bipy)]^-$ at the same cathodic potential (detectable under argon, cf. Figure SI-4b, Supporting Information), triggering electrocatalytic reduction of CO_2. Inset: the $^{13}CO_2$ satellite peak used as a reference. Conditions: CO_2-saturated THF/TBAH containing 5% TFE, an OTTLE cell (Pt mesh cathode), λ_{exc} = 405 nm (irradiation times in minutes), T = 298 K.

The related complex, $[Mn(CO)_3(bipy)(OTf)]$ (OTf = $CF_3SO_3^-$) was also investigated during the course of this study. This derivative is reducible at a significantly less negative cathodic potential compared to R1 of **1**, viz. $E_{p,c}$ = -1.32 V vs Fc/Fc^+ ($\Delta E_{p,c}$ = +0.59 V) , see Figure SI-11 (Supporting Information).The latter value is actually less negative than the anodic potential for the reoxidation of $[Mn(CO)_3(bipy)]^-$, viz. $E_{p,a}$ = -1.64 V vs Fc/Fc^+, which represents the limiting value for the dimer-based photo-assisted cathodic process. Thus, in order to keep the 5-coordinate anion stable during the photo-assisted measurement it was necessary to set the potential slightly more negative of R1, that is, in the vicinity of R2' (Scheme 1). Despite the less negative reduction potential, spectroelectrochemistry confirms that the Mn-OTf complex (v(CO) at 2043 and 1943br cm^{-1}) converts again to $[Mn(CO)_3(bipy)]_2$ at R1, which reduces further at R(D) to give the stable 5-coordinate anion (Figure SI-12, Supporting Information). Importantly, $[Mn(CO)_3(bipy)]^-$ can also be produced with the photo-assistance already at R2' (around -1.55 V vs Fc/Fc^+) from transient $[Mn(CO)_3(bipy)]$ (Figure SI-13, Supporting Information).

Photo-assisted Electrochemical Reduction of $[Mo(CO)_4(6,6'\text{-dmbipy})]$ (2)

The electrochemical activation of **2** under both Ar and CO_2 has already been extensively described elsewhere, using again a combination of CV and IR/UV-vis spectroelectrochemistry.[19] To refresh, on the cathodic scan two separate reduction steps can be observed (Figure SI-14, Supporting Information). The first one (R1) is the reversible $1e^-$ reduction producing stable $[Mo(CO)_4(6,6'\text{-dmbipy})]^{\bullet-}$. In THF/TBAH at a Pt cathode, this process lies at $E_{1/2}$ = -2.13 V vs Fc/Fc^+. The subsequent irreversible reduction of the 6-coordinate radical anion at $E_{p,c}$ = -

2.71 V (R2) produces the 5-coordinate dianion, $[Mo(CO)_3(6,6'\text{-dmbipy})]^{2-}$. On the reverse anodic scan, the wave O2' is observed at $E_{p,a}$ = -2.41 V, which corresponds to 1e⁻ oxidation of the 5-coordinate dianion to the corresponding reactive 5-coordinate radical anion. At an Au cathodic surface, the catalytic CO_2 reduction does not start at R2 but already in the vicinity of the R2'/O2' redox couple of the tricarbonyl species. As before, infrared spectroelectrochemistry offers clarity on the nature of the reduced species (Figure SI-15, Supporting Information). At R1, the low energy shift of the four ν(CO) bands of the parent cis-isomer at 2014, 1899, 1879 and 1836 cm^{-1} become red-shifted by roughly 30 cm^{-1} to 1994, 1873, 1844 and 1799 cm^{-1}. The retention of the ν(CO) tetracarbonyl band pattern advocates for the stable radical anionic structure. The subsequent cathodic conversion from the 6-coordinate radical anion to $[Mo(CO)_3(6,6'\text{-dmbipy})]^{2-}$ (formally a π-delocalized $(CO)_3Mo^{-I}$–bipy⁻ species) at R2 is proved by the appearance of three low-energy ν(CO) bands at 1843, 1718 and 1701 cm^{-1}. Importantly, the photo-assisted electrochemical reduction of **2** (Figure 4), when irradiating the primary 6-coordinate radical anion with 365-nm light, generates the 5-coordinate dianion already at R2', that is, about 400 mV less negatively than the standard electrolysis at the cathodic wave R2, regardless of the metallic cathodic surface – at Pt (Figure 4), Au (Figure SI-16, Supporting Information) or Cu (Figure SI-17, Supporting Information). This behavior presents a significant advantage over the standard cathodic path, where only the Au cathodic surface has been shown to promote limited CO dissociation from $[Mo(CO)_4(6,6'\text{-dmbipy})]^{\bullet-}$, opening the chance for the 5-coordinate dianion to be produced at R2'. In this study, only the 365-nm irradiation of the tetracarbonyl radical anion was attempted, as this wavelength has the best cross-sectional overlap with the anticipated MLCT band of interest, see the UV-vis spectrum of the radical anion (Figure SI-18, Supporting Information). Unexpectedly, the 5-coordinate dianion itself is photoreactive at λ_{exc} = 365 nm (Figure SI-19, Supporting Information) under the applied cathodic potential of R2, converting quickly to a secondary, yet unassigned species absorbing at 1864 and 1712br cm^{-1}. The small shift and little change in the ν(CO) band pattern point to a species having a similar molecular and electronic structure as original $[Mo(CO)_3(6,6'\text{-dmbipy})]^{2-}$. In the presence of CO_2, there is no catalytic response of **2** when reduced at R1/R2' using a Pt cathode, on the standard electrochemical route (Figure SI-20, Supporting Information). Only when the cathodic potential is swept to R2, the catalytic reduction of CO_2 becomes evidenced by the major production of CO accompanied by bicarbonate (1676 and 1641 cm^{-1}) and subordinate formate (1607 cm^{-1}).[19]

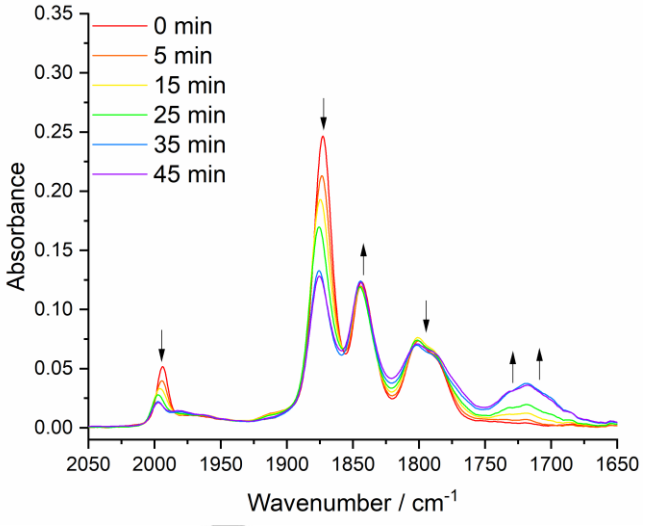

Figure 4. IR SEC monitoring of the photo-assisted electrochemical conversion of $[Mo(CO)_4(6,6'\text{-dmbipy})]^{\bullet-}$ (↓), pre-formed from **2** at the cathodic wave R1, to the 5-coordinate dianion, $[Mo(CO)_3(6,6'\text{-dmbipy})]^{2-}$ (↑) at the cathodic wave R2'. Conditions: Ar-saturated THF/TBAH, an OTTLE cell (Pt mesh cathode), λ_{exc} = 365 nm (irradiation times in minutes), T = 298 K.

The formation of an inactive tetracarbonyl complex (ν(CO) at 2005, 1885, 1867 and 1829 cm^{-1}) is ascribed to moisture present in the CO_2-saturated electrolyte, and is representing the major deactivation path for the catalyst $[Mo(CO)_3(6,6'\text{-dmbipy})]^{2-}$. The latter wavenumbers are larger compared to $[Mo(CO)_4(6,6'\text{-dmbipy-H})]^-$ under argon[19] (Table 1), which may reflect some interaction of the protonated anion with CO_2. The minor ν(CO) band at 1920 cm^{-1} detected during the experiment is diagnostically important for the catalytic process taking place.[25] Using the photo-assisted electrochemical reduction (Figure 5), an almost identical set of CO_2-originated products form already at R2', again proving the advantage of this method. However, the ratio of the products is changed slightly as less formate seems to form along this route. Once formed, the 5-coordinate dianion reacts rapidly with CO_2, and the same also applies for the photoproduct detected during the experiment under argon, which, differently from **1**, eliminates parallel photoreactivity as a drawback in this case. Differently from the standard electrochemical reduction at R2 under CO_2, the inactive tetracarbonyl complex absorbing at 2005, 1885, 1867 and 1829 cm^{-1} was not observed, which ultimately led to a more efficient conversion of CO_2. Notably, a different tetracarbonyl product formed in the course of the photo-assisted electrocatalysis, with ν(CO) at 1980, 1864, 1831 and 1784 cm^{-1}. The values are smaller than the ν(CO) wavenumbers of precursor $[Mo(CO)_4(6,6'\text{-dmbipy})]^{\bullet-}$ (1994, 1873, 1844 and 1799 cm^{-1}). The identity of this resulting reduced tetracarbonyl species is unknown as yet. The growing ν(CO) band at 1920 cm^{-1}, which is marking the electrocatalytic reduction of CO_2 at R2 in Figure SI-20 (Supporting Information) is also seen for the photoassisted process at R2' (Figure 5, denoted with asterisk).

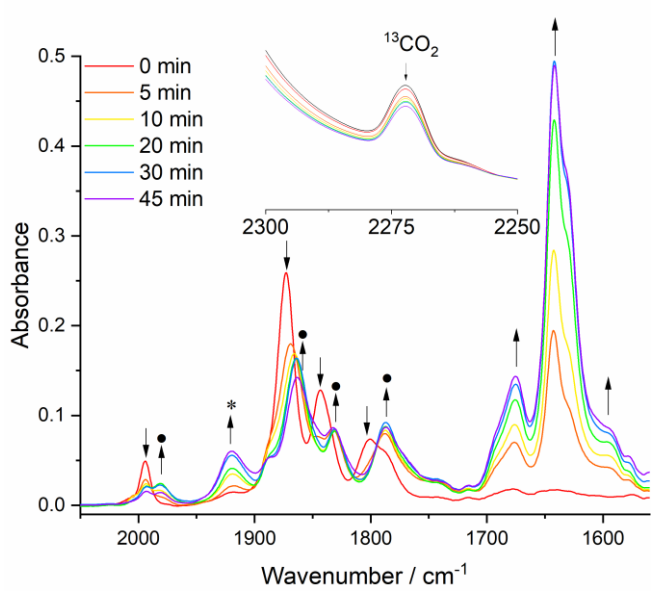

Figure 5. IR SEC monitoring of the photo-assisted electrochemical reduction of $[Mo(CO)_4(6,6'\text{-dmbipy})]^{\bullet-}$ ($\downarrow$) at R2' to transient $[Mo(CO)_3(6,6'\text{-dmbipy})]^-$ that reduces a part of CO_2 to CO (accompanied by bicarbonate) and free formate. The labels $^\bullet$ denote an ultimate tetracarbonyl product. Inset: the $^{13}CO_2$ satellite peak serving as a reference. Conditions: CO_2-saturated THF/TBAH, an OTTLE cell (Pt mesh cathode), λ_{exc} = 365 nm (irradiation times in minutes), T = 298 K.

Conclusions

We have shown how combined photo- and electrochemical reactivity of catalyst precursors can be exploited in attempts to specifically target a high-overpotential catalyst of CO_2 reduction along the reduction path of two reference parent complexes of Earth-abundant transition metals, viz. $[Mn(CO)_3(bipy)Br]$ and $[Mo(CO)_4(6,6'\text{-dmbipy})]$. In terms of the required overpotential, the dissociative photoexcitation of the 1e$^-$ reduced intermediates, viz. $[Mn(CO)_3(bipy)]_2$ and $[Mo(CO)_4(6,6'\text{-dmbipy})]^{\bullet-}$, respectively, assists the electrochemical reduction by replacing the second cathodic step at a highly negative electrode potential, thereby effectively 'locking' the 2e$^-$-reduced catalyst in the active form at (Mn) or close to (Mo) the parent reduction potential, or more precisely close to its reoxidation potential, which is almost unheard of for these catalysts. Despite the positives, the behavior is obviously complex, and more work is needed to understand particularly the details of photochemistry behind the cleavage of the Mn–Mn and Mo–CO bonds, respectively, in the 1e$^-$ reduced catalyst precursors. There is a clear potential for the powerful photo-assisted alternative to the exclusively electrocatalytic cathodic process. This pilot study demonstrates that the onset of the electrocatalytic reduction of CO_2 to CO can be shifted to a lower energy significantly, depending on the redox properties of the catalyst. The presented exploratory work is believed to serve as an inspiration for the community to search for other cases where photo-assisted electrochemical activation may successfully be applied to trigger, and facilitate, electron-transfer-based catalytic processes.

Supporting Information

The Supporting Information is available free of charge on the website at DOI: Contents: Full experimental details, supplementary cyclic voltammograms, supplementary spectroelectrochemical experiments under Ar and CO_2.

Experimental Section

Detailed Materials and Methods sections can be found in the Supporting Information. $[Mn(CO)_3(2,2'\text{-bipyridine})Br]$ (**1**) (Ref. [10]), $[Mn(CO)_3(2,2'\text{-bipyridine})(OTf)]$ (Ref. [45]) and $[Mo(CO)_4(6,6'\text{-dimethyl-2,2'-bipyridine})]$ (**2**) (Ref. [19]) were synthesised in house according to the established literature procedures.

Author Information

Corresponding Author

*Email: f.hartl@reading.ac.uk

ORCID

František Hartl: 0000-0002-7013-5360

Acknowledgements

This work was jointly funded by the EPSRC and Spectroelectrochmistry Reading, a spin-out company of the University of Reading (F.H.) - project EPSRC-DTP GS16-014.

Conflict of Interest

Authors declare no competing financial interest.

Keywords: Earth-Abundant Metal • Spectroelectrochemistry • Electrocatalytic CO_2 Reduction • Electrocatalyst • Photocatalyst • Photo-assisted electrochemistry

References

[1] N. Armaroli, V. Balzani, *Chem. Eur. J.* **2016**, *22*, 32–57.

[2] R. Francke, B. Schille, M. Roemelt, *Chem. Rev.* **2018**, *118*, 4631–4701.

[3] K. Li, X. An, K. H. Park, M. Khraisheh, J. Tang, *Catal. Today* **2014**, *224*, 3–12.

[4] J. Zhao, X. Wang, Z. Xu, J. S. C. Loo, *J. Mater. Chem. A* **2014**, *2*, 15228.

[5] K. A. Grice, *Coord. Chem. Rev.* **2017**, *336*, 78–95.

[6] N. Elgrishi, M. B. Chambers, X. Wang, M. Fontecave, *Chem. Soc. Rev.* **2017**, *46*, 761–796.

[7] C. Jiang, A. W. Nichols, C. W. Machan, *Dalton Trans.* **2019**, *48*,

9454–9468.

[8] J. Hawecker, J.-M. Lehn, R. Ziessel, *J. Chem. Soc. Chem. Commun.* **1984**, *984*, 328.

[9] H. Takeda, K. Koike, H. Inoue, O. Ishitani, *J. Am. Chem. Soc.* **2008**, *130*, 2023–2031.

[10] M. Bourrez, F. Molton, S. Chardon-Noblat, A. Deronzier, *Angew. Chem. Int. Ed.* **2011**, *50*, 9903–9906.

[11] M. Bourrez, M. Orio, F. Molton, H. Vezin, C. Duboc, A. Deronzier, S. Chardon-Noblat, *Angew. Chem. Int. Ed.* **2014**, *53*, 240–243.

[12] J. M. Smieja, M. D. Sampson, K. A. Grice, E. E. Benson, J. D. Froehlich, C. P. Kubiak, *Inorg. Chem.* **2013**, *52*, 2484–2491.

[13] M. Stanbury, J.-D. Compain, M. Trejo, P. Smith, E. Gouré, S. Chardon-Noblat, *Electrochim. Acta* **2017**, *240*, 288–299.

[14] M. Stanbury, J.-D. Compain, S. Chardon-Noblat, *Coord. Chem. Rev.* **2018**, *361*, 120–137.

[15] D. C. Grills, M. Z. Ertem, M. McKinnon, K. T. Ngo, J. Rochford, *Coord. Chem. Rev.* **2018**, *374*, 173–217.

[16] H. Rao, L. C. Schmidt, J. Bonin, M. Robert, *Nature* **2017**, *548*, 74–77.

[17] R. B. Ambre, Q. Daniel, T. Fan, H. Chen, B. Zhang, L. Wang, M. S. G. Ahlquist, L. Duan, L. Sun, *Chem. Commun.* **2016**, *52*, 14478–14481.

[18] C. Costentin, M. Robert, J. M. Savéant, *Acc. Chem. Res.* **2015**, *48*, 2996–3006.

[19] J. O. Taylor, R. D. Leavey, F. Hartl, *ChemElectroChem* **2018**, *5*, 3155–3161.

[20] J. O. Taylor, F. L. P. Veenstra, A. M. Chippindale, M. J. Calhorda, F. Hartl, *Organometallics* **2019**, *38*, 1372–1390.

[21] M. L. Clark, K. A. Grice, C. E. Moore, A. L. Rheingold, C. P. Kubiak, *Chem. Sci.* **2014**, *5*, 1894–1900.

[22] F. Franco, C. Cometto, F. Sordello, C. Minero, L. Nencini, J. Fiedler, R. Gobetto, C. Nervi, *ChemElectroChem* **2015**, *2*, 1372–1379.

[23] L. Rotundo, C. Garino, R. Gobetto, C. Nervi, *Inorg. Chim. Acta* **2018**, *470*, 373–378.

[24] K. A. Grice, C. Saucedo, *Inorg. Chem.* **2016**, *55*, 6240–6246.

[25] J. Tory, B. Setterfield-Price, R. A. W. Dryfe, F. Hartl, *ChemElectroChem* **2015**, *2*, 213–217.

[26] J. Tory, G. Gobaille-Shaw, A. M. Chippindale, F. Hartl, *J. Organomet. Chem.* **2014**, *760*, 30–41.

[27] F. P. A. Johnson, M. W. George, F. Hartl, J. J. Turner, *Organometallics* **1996**, *15*, 3374–3387.

[28] G. Neri, P. M. Donaldson, A. J. Cowan, *Phys. Chem. Chem. Phys.* **2019**, *21*, 7389–7397.

[29] M. D. Sampson, C. P. Kubiak, *J. Am. Chem. Soc.* **2016**, *138*, 1386–1393.

[30] M. D. Sampson, A. D. Nguyen, K. a. Grice, C. E. Moore, A. L. Rheingold, C. P. Kubiak, *J. Am. Chem. Soc.* **2014**, *136*, 5460–5471.

[31] G. J. Stor, S. L. Morrison, D. J. Stufkens, A. Oskam, *Organometallics* **1994**, *13*, 2641–2650.

[32] T. J. Meyer, J. V. Caspar, *Chem. Rev.* **1985**, *85*, 187–218.

[33] M. Sarakha, G. Ferraudi, *Inorg. Chem.* **2002**, *38*, 4605–4607.

[34] H. Cho, K. Hong, M. L. Strader, J. H. Lee, R. W. Schoenlein, N. Huse, T. K. Kim, *Inorg. Chem.* **2016**, *55*, 5895–5903.

[35] D. J. Stufkens, T. van der Graaf, G. J. Stor, A. Oskam, *Coord. Chem. Rev.* **1991**, *111*, 331–336.

[36] E. Fujita, J. T. Muckerman, *Inorg. Chem.* **2004**, *43*, 7636–7647.

[37] Y. Hayashi, S. Kita, B. S. Brunschwig, E. Fujita, *J. Am. Chem. Soc.* **2003**, *125*, 11976–11987.

[38] G. Neri, P. M. Donaldson, A. J. Cowan, *J. Am. Chem. Soc.* **2017**, *139*, 13791–13797.

[39] J. Vichova, F. Hartl, A. Vlcek, *J. Am. Chem. Soc.* **1992**, *114*, 10903–10910.

[40] S. Záliš, I. R. Farrell, A. Vlček, *J. Am. Chem. Soc.* **2003**, *125*, 4580–4592.

[41] A. Vlček, *Coord. Chem. Rev.* **2002**, *230*, 225–242.

[42] W. Kaim, S. Kohlmann, A. J. Lees, T. L. Snoeck, D. J. Stufkens, M. M. Zulu, *Inorg. Chim. Acta* **1993**, *210*, 159–165.

[43] F. Hartl, P. Rosa, L. Ricard, P. Le Floch, S. Záliš, *Coord. Chem. Rev.* **2007**, *251*, 557–576.

[44] In ionic liquid, the decomposition pathway is exacerbated to the point where hardly any dimer is converted to the 5-coordinate anion. This may be due to the enhanced dipole in this unusual solvent.

[45] E. Hevia, J. Pérez, L. Riera, V. Riera, D. Miguel, *Organometallics* **2002**, *21*, 1750–1752.

Entry for the Table of Contents (Please choose one layout)

Layout 1:

RESEARCH ARTICLE

IR spectroelectrochemistry has unravelled the potential for photo-assisted electrochemical reduction of $[Mn(CO)_3(bipy)Br]$ and $[Mo(CO)_4(6,6'-dmbipy)]$ for triggering electrocatalytic reduction of CO_2 at lower overpotentials. Utilizing the Mn–Mn and Mo–CO dissociative photochemistry of the $1e^-$ reduced species, respectively, the active 5-coordinate catalysts already operate near the parent cathodic waves, in a marked difference from the purely electrochemical routes.

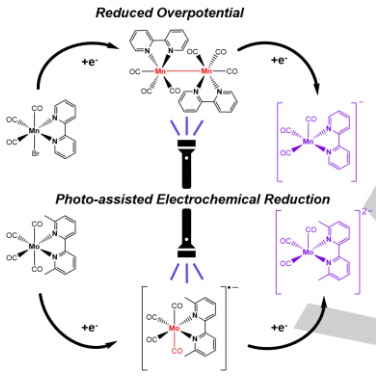

*Author(s), Corresponding Author(s)**

Page No. – Page No.

Title